



- 1 Threshold Atmospheric Electric Fields for Initiating Relativistic Runaway Electron
- 2 Avalanches: Theoretical Estimates and CORSIKA Simulations
- 3 Ashot Chilingarian*, Liza Hovhannisyan, Mary Zazyan
- 4 A I Alikhanyan national lab (Yerevan Physics Institute), Alikhanyan Brothers 2, Yerevan
- 5 36, Armenia
- 6 *corresponding author chili@aragats.am

7 Abstract

- 8 We examine the threshold Atmospheric Electric Field (Eth) needed to initiate a runaway
- 9 avalanche process in Earth's atmosphere. We compare the traditional, thirty-year-old
- theoretical threshold value with its recently updated value, along with the threshold
- derived from CORSIKA-simulated avalanches (Ez). The altitude dependence of these
- 12 threshold values is analyzed, considering changes in air density and their effects on
- 13 avalanche development. This study is vital for understanding high-energy atmospheric
- phenomena in both the lower and upper atmosphere, including thunderstorm ground
- 15 enhancements (TGEs) and gamma glows, as well as for refining AEF models based on
- 16 particle flux measurements.

17 Short Summary

- 18 Thunderstorms can accelerate particles in the atmosphere, producing bursts of radiation at
- 19 the ground. We investigated how strong the electric field inside a cloud must be to start
- 20 such events. Using advanced computer simulations and comparing with measurements
- 21 from mountain stations, we found that fields must be stronger than earlier theory
- 22 suggested. Our results improve understanding of storm electricity and its role in natural
- 23 radiation.

24 Highlights

- Introduces a refined framework for determining threshold atmospheric electric fields (Eth) needed to initiate relativistic runaway electron avalanches (RREAs) and thunderstorm ground enhancements (TGEs).
- Compares classical (Eth ≈ 2.80 × n) and updated (Eth ≈ 2.67 × n) theoretical
 thresholds with altitude-dependent thresholds derived from CORSIKA
 simulations.
- Demonstrates that realistic avalanche development requires fields 15–22% stronger than theoretical values, depending on altitude and air density.
- Provides a reproducible simulation methodology for integrating experimental particle flux measurements into atmospheric electricity models across multiple research stations.





36 Introduction

- 37 Free electrons are abundant in the troposphere. The altitude where their density reaches
- 38 its highest point—called the Regener–Pfotzer maximum—depends on various factors,
- 39 including the geomagnetic cutoff rigidity (Rc), the type of particles being measured, and
- 40 the phase and strength of the solar cycle. Recent observations, supported by PARMA4.0
- 41 calculations (Sato, 2016), show that at middle to low latitudes (Rc = 3-8 GV), the highest
- 42 flux of charged particles occurs at altitudes around 12–14 km (see Fig. 4 in Ambrozova et
- 43 al., 2023).
- 44 Atmospheric electric fields (AEFs) generated by thunderstorms transfer energy to free
- electrons, accelerate them, and, under certain conditions, induce electron-photon
- 46 avalanches. In 1992, Gurevich, Milikh, and Roussel-Dupré identified the conditions
- 47 necessary for extensive multiplication of electrons from each energetic seed electron
- 48 injected into a strong AEF region (Gurevich et al., 1992). This process is known as the
- 49 Relativistic Runaway Electron Avalanche (RREA; Babich et al., 2001; Alexeenko et al.,
- 50 2002). A numerical approach for solving the relativistic Boltzmann equation for runaway
- 51 electron beams (Symbalisty et al., 1998) aids in estimating the threshold AEF (Babich et
- 52 al., 2001; Dwyer et al., 2003) required to trigger RREA. As demonstrated by GEANT4
- and CORSIKA simulations (Chilingarian et al., 2012, 2022), the RREA process is a
- 54 threshold phenomenon, with avalanches initiating when the atmospheric AEF exceeds a
- 55 certain threshold, which depends on the air density. The AEF must also be sufficiently
- 56 extended to support the growth of avalanches. At standard temperature and pressure in
- dry air at sea level, Eth $\approx 2.80 * n \text{ kV/cm}$, where air density n is relative to the
- 58 International Standard Atmosphere (ISA) sea-level value (see the recent update of the
- threshold energy Eth $\approx 2.67 * n \text{ kV/cm}$ in Dwyer and Rassoul, 2024).
- 60 This threshold field is slightly higher than the breakeven field, which corresponds to the
- 61 electron energy at which minimum ionization occurs. If electrons traveled exactly along
- 62 AEF lines, it would define the threshold for runaway electron propagation and the start of
- avalanche formation. However, the paths of electrons deviate due to Coulomb scattering
- 64 with atomic nuclei and Møller scattering with atomic electrons, causing deviations from
- 65 the near-vertical AEF. Additionally, secondary electrons produced by Møller scattering
- are not generated along the field line; therefore, AEFs 10-20% stronger are required for
- 67 electrons to run away and trigger an avalanche.



68 1. Corsika simulations of RREAs reaching on Aragats stations

- 69 To understand how avalanches develop in an electrified atmosphere and to compare the
- 70 new and updated Eth with the particle intensity growth, we used the CORSIKA code
- 71 (Heck et al., 1998), version 7400, which takes into account the effect of AEFs on particle

https://doi.org/10.5194/egusphere-2025-4153 Preprint. Discussion started: 5 October 2025 © Author(s) 2025. CC BY 4.0 License.





- 72 transport (Butnik et al., 2010). The growth of RREA definitely increases the cloud's
- 73 electrical conductivity. Numerous studies (Marshall et al., 1995; Stolzenburg et al., 2007)
- have indicated that lightning flashes occur after the RREA threshold exceeds 20-30%.
- 75 RREA simulation codes do not include a lightning initiation mechanism. Therefore, one
- 76 can artificially raise the AEF strength beyond a realistic value to produce billions of
- avalanche particles; however, this approach lacks physical justification. As a result, we
- 78 do not test AEFs stronger than 2.2 kV/m at altitudes of 3-6 km. The RREA simulation
- 79 was performed for vertical seed electrons with a uniform AEF that exceeded the E_{th} by a
- 80 few tens of percent. An introduced fixed uniform AEF shifts the surplus to E_{th} at different
- 81 heights by different percent, corresponding to air density. The seed electron energy
- 82 spectrum was based on the EXPACS WEB calculator (Sato, 2018), following a power
- law with an index of 1.173 for energies from 1 to 300 MeV. During TGE events on
- 84 Aragats, the typical distance to the cloud base is estimated to be 25–200 m (see Fig. 17 in
- 85 Chilingarian et al., 2020); therefore, in our simulations, particle propagation continued in
- 86 dense air for an additional 25, 50, 100, and 200 meters before detection. The simulations
- 87 included 1,000 to 10,000 events for AEF strengths from 1.55 to 2.5 kV/cm. Electron and
- gamma-ray propagation was tracked until their energies dropped to 0.05 MeV. The
- 89 CORSIKA code models RREA development, calculating the number of electrons and
- gamma rays at various stages within the AEF, every 200 m.
- 91 Besides the Aragats and Nor Amberd research stations on the slopes of Mt. Aragats in
- 92 Armenia, we also conducted simulations for Slovakian and Chinese research stations at
- 93 Lomnicky Stit and the Tibetan plateau. LHAASO (Large High Altitude Air Shower
- 94 Observatory) is situated at 4410 meters above sea level. It provides an ideal platform for
- 95 studying atmospheric particle acceleration due to its thin atmosphere and high likelihood
- 96 of runaway electron avalanche formation. We present CORSIKA simulation results
- 97 showing increases in electron and photon fluxes under AEF strengths ranging from 1.55
- 98 to 1.9 kV/m. The number of electrons and photons was recorded at depths ranging from
- 99 6510 meters to 4510 meters.
- 100 Lomnický Štít is located at an altitude of 2630 meters in Slovakia. CORSIKA simulations
- 101 were performed for various vertical AEFs ranging from 1.9 to 2.3 kV/cm. The number of
- electrons and photons was recorded at depths ranging from 4734 meters to 2734 meters.
- 103 Significant increases in flux were observed with stronger fields, confirming the
- development of robust RREA. Saturation trends in the growth of electrons and photons
- suggest that the threshold field, Eth, at Lomnický Štít is approximately 2.3 kV/cm. These
- 106 results support earlier findings from Aragats and Nor Amberd and emphasize the altitude
- dependence of Eth. Due to the thinner air, at Lhasso, the TGEs occurred at a much lower
- 108 value of 1.7 kV/m.
- 109 In Figures 1-4, we display the development of RRE avalanches at different atmospheric
- depths and for various physically justified strengths of the AEF. The curves are scaled for
- a single seed electron for easier comparison with experimentally measured intensities.
- For each lower value of AEF, we observe saturation of the particle flux; the RREA





process attenuates before reaching the observation level (see the red and yellow curves in Figs. 1-4).

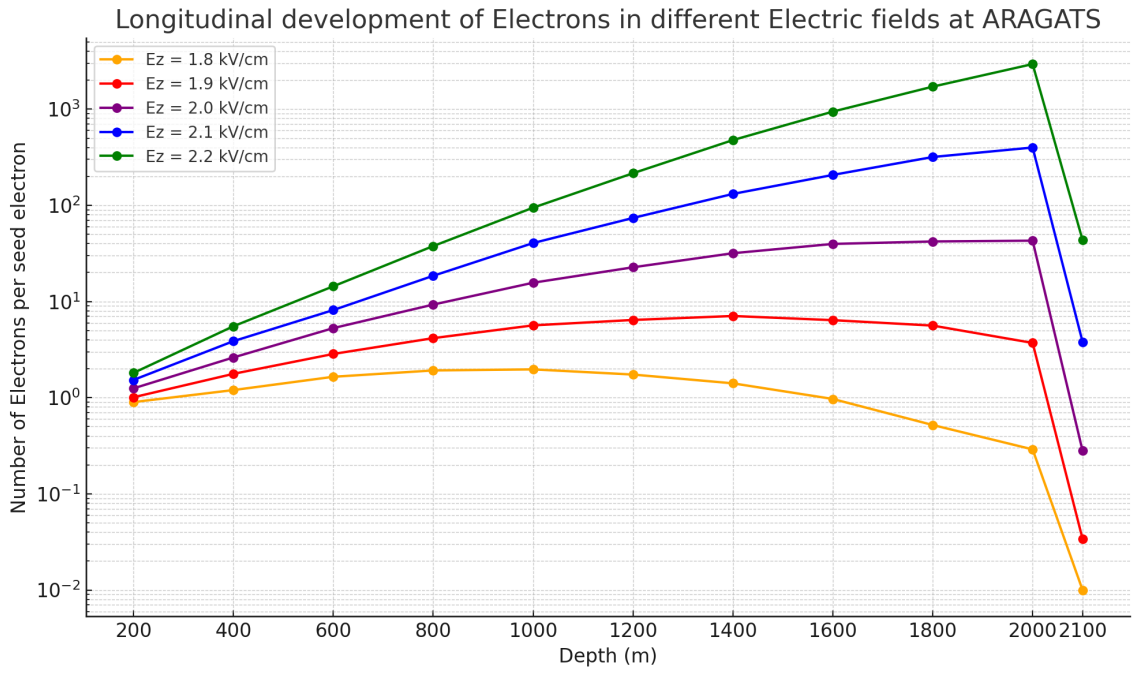


Figure 1. Development of the RRE avalanche in the atmosphere. The avalanche started at 5400 meters above sea level, which is 2100 meters higher than the Aragats station. The number of avalanche particles is calculated every 200 meters. After leaving the AEF, the movement of avalanche particles is tracked for an additional 100 meters before reaching the station.



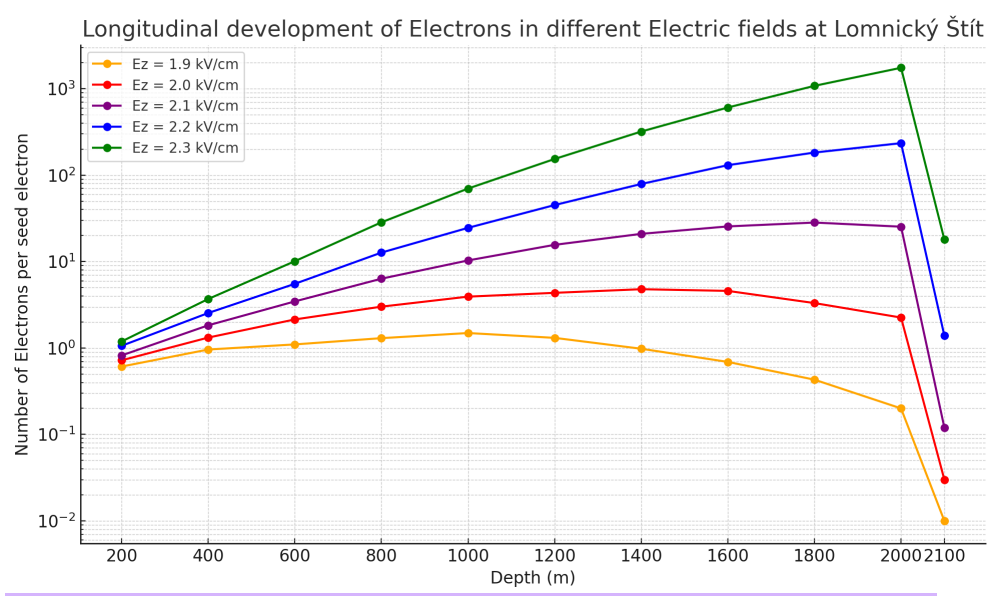


Figure 2. Development of the RRE avalanche in the atmosphere. The avalanche started at 4730 meters above sea level, which is 2100 meters higher than the Lomnicky Stit station. The number of avalanche particles is calculated every 200 meters. After leaving the AEF, the movement of avalanche particles is tracked for an additional 100 meters before reaching the station.

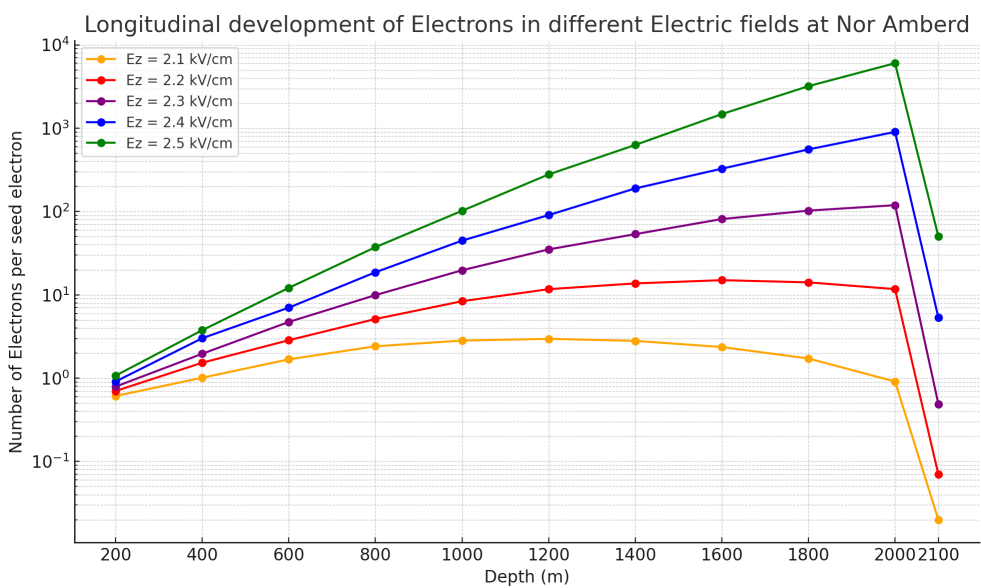


Figure 3. Development of the RRE avalanche in the atmosphere. The avalanche began at 4100 m a.s.l. (0 meters depth), which is 2100 meters above the Nor Amberd station. The number of avalanche particles is calculated every 200 meters. After





exiting the AEF, the propagation of avalanche particles is tracked for an additional 100 meters before reaching the station.

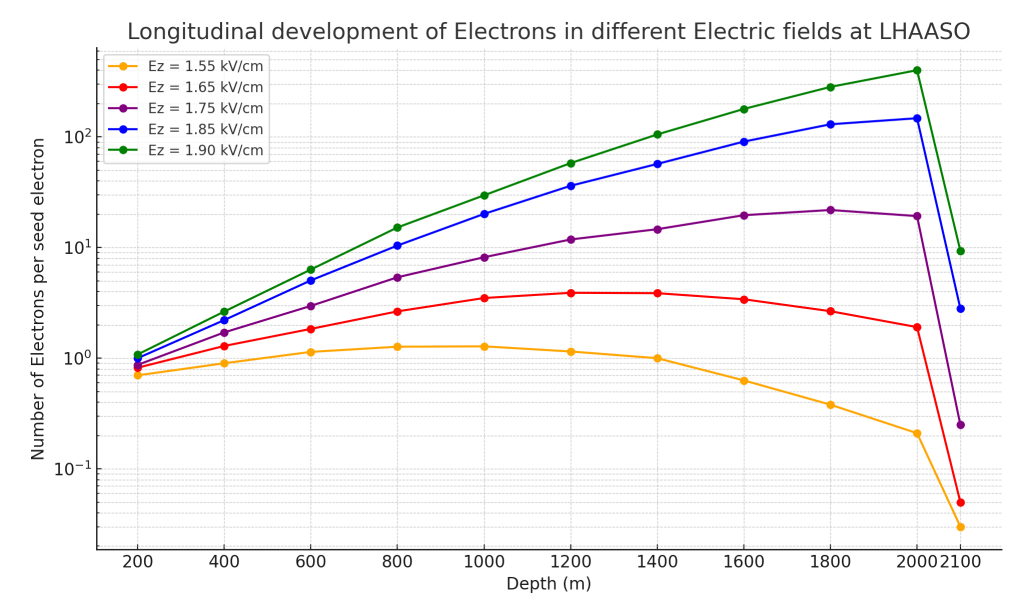


Figure 4. Development of the RRE avalanche in the atmosphere. The avalanche started at 6510 meters above sea level, which is 2100 meters higher than the LHAASO station. The number of avalanche particles is calculated every 200 meters. After leaving the AEF, the movement of avalanche particles is tracked for an additional 100 meters before reaching the station.

We estimate the "simulated" thresholds, E_z values, at the heights at which the amount of avalanche particles stops rising, as shown in Fig. 5.





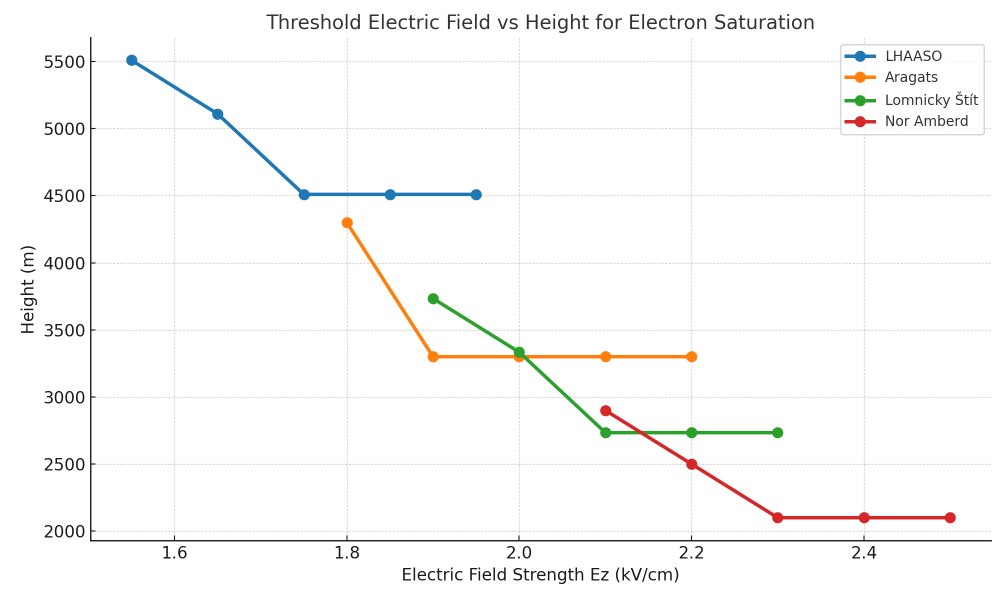


Figure 5. The electric field strengths (Eth) at the point when the RREA particle flux began to decline for 4 stations located at altitudes ranging from 2000 to 4100 meters.

In Figure 6 and Table 1, we compare the "simulated" threshold Ez with the theoretical ones. Simulations show higher values than theoretical estimates, especially for high Eth values (low altitudes) at all four research stations. The relative air density n is calculated using an exponential atmospheric model. Threshold fields are computed as $2.67 \times n$ and $2.80 \times n$, representing the updated and theoretical thresholds, respectively. The percentage of enhancement indicates how much the applied field exceeds the theoretical thresholds. Strong AEFs, where the cascade did not attenuate, were not included in the table.





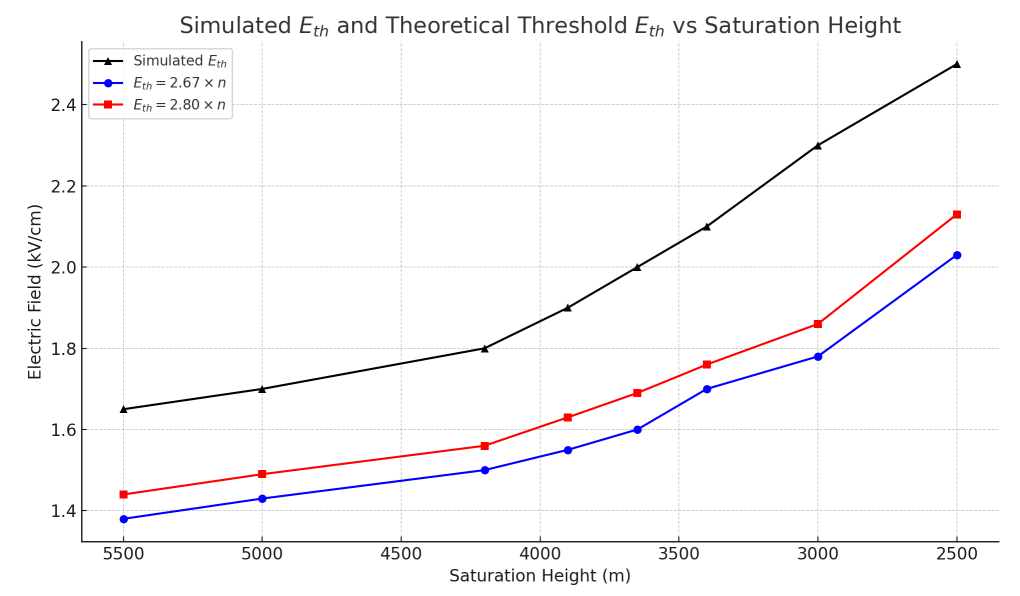


Figure 6. The dependence of the heights in the atmosphere and the corresponding threshold AEF to start RREA for theoretical and simulated values.

Table 1. Excess of E_z over $E_{th}.$ Stopping altitudes and theoretical threshold field comparisons for heights 2500- 5550 m.

Input Ez	Enhancement	n	2.67 × n	2.80 × n	Rel.	Rel.	Site
(kV/cm)	Stops at h(m)	(relative	(kV/cm)	(kV/cm)	Excess.	Excess.	
		density)			(%)	(%)	
					(2.80)	(2.67)	
1.55	5510	0.465	1.24	1.30	19.0	24.8	LHAASO
							(4400 m)
1.65	5110	0.492	1.31	1.38	19.8	25.7	LHAASO
							(4400 m)
1.8	4200.0	0.558	1.49	1.56	15.2	20.8	Aragats
							(3200 m)
1.9	3900.0	0.582	1.55	1.63	16.6	22.3	Aragats
							(3200 m)
1.9	3734	0.595	1.59	1.67	14.0	19.5	Lomnicky
							Štít (2630
							m)
2.0	3334	0.629	1.68	1.76	13.5	19.0	Lomnicky
							Štít (2630
							m)





2.1	2700.0	0.687	1.84	1.92	9.1	14.4	Nor
							Amberd
							(2000 m)
2.2	2500.0	0.707	1.89	1.98	11.2	16.6	Nor
							Amberd
							(2000 m)

164

165

166

167

168

169 170

171

172

173 174

175

176 177

178

2. Discussion and conclusion

Although both the classical threshold field (Eth $\approx 2.80 \times n \, kV/cm$) and its updated version (Eth $\approx 2.67 \times \text{n kV/cm}$) are derived under idealized assumptions, the difference between them results from refinements in modeling particle energy loss processes. The earlier estimate of 2.80 × n was based on basic energy balance considerations using older ionization loss models and assumed monoenergetic electrons. This threshold is slightly above the breakeven field, where energy gain equals average energy loss. The updated 2.67 × n value, introduced by Dwyer and Rassoul (2024), incorporates more accurate relativistic Boltzmann solutions, improved ionization and bremsstrahlung cross-sections, and a probabilistic treatment of runaway thresholds across realistic energy spectra. While both thresholds assume idealized, field-aligned electron motion in a uniform medium, the updated value is physically more consistent. It predicts a slightly lower field strength needed for initial runaway. However, CORSIKA simulations show that this refined threshold is insufficient for sustained avalanche growth under real atmospheric conditions due to scattering and finite path effects. Moreover, it deviates more from the simulated value than the "classical" 30-year-old estimate.

179 180 181

182

183

184 185

186

187

188 189

190 191

Multiple physical processes act to inhibit ideal runaway propagation. Coulomb scattering with atmospheric nuclei and Møller scattering with electrons cause substantial angular deflection and energy redistribution. Secondary electrons are not generated strictly along the field direction, and many lose energy before gaining sufficient momentum to continue avalanche growth. As a result, electrons must be accelerated in stronger-than-threshold fields to overcome these losses and maintain avalanche conditions.

CORSIKA simulations, which incorporate all major interaction mechanisms—including Coulomb and Møller scattering, bremsstrahlung losses, finite propagation distances, and realistic secondary cosmic ray spectra—demonstrate that avalanches only fully develop when the applied field exceeds the theoretical threshold by a measurable margin. For the updated 2.67 × n value, we observe a required excess of approximately 20-22% at the Aragats station (\sim 3200–4200 m a.s.l.), whereas for the classical 2.80 × n threshold, the

192 193 excess is typically 15-17%.

194 Interestingly, this required excess decreases with increasing air density, as observed in 195 the Nor Amberd simulations. At lower altitudes ($\sim 2500-2700$ m a.s.l.), the difference

196 between the applied and threshold fields is reduced: only 14–16% above 2.67 × n, and

about 9–11% above $2.80 \times n$. This trend can be explained as follows: 197

198 In denser air, the chances of energy loss interactions increase, but so does the likelihood 199 of electron multiplication through ionization and bremsstrahlung over shorter distances.

200 The avalanche can develop more quickly because seed electrons encounter more target





201 atoms in a given path length. As a result, the necessary "headroom" above the threshold 202 field for sustained multiplication is smaller. Simply put, the efficiency of avalanche 203 formation improves in denser air, even though the absolute threshold field is higher. This 204 results in a smaller relative excess being required above the theoretical threshold. 205 206 Therefore, although the threshold field scales linearly with air density, the required 207 enhancement factor does not. It decreases with increasing density due to a balance 208 between energy loss and multiplication processes, all of which are faithfully captured in 209 the CORSIKA simulation framework. This emphasizes the importance of altitude-210 dependent analysis in interpreting Thunderstorm Ground Enhancements (TGEs) and suggests that scaling laws based solely on density may overlook subtler effects arising 211 from atmospheric structure and shower development dynamics. 212 213 214 Code and data availability 215 Data archive on TGE event is reposted on the Mendelay site at 216 217 https://doi.org/10.17632/8gtdbch59z (Chilingarian et al., 2024). Data archive on CORSIKA simulations (RREA development in the atmosphere above 4 218 219 sites) is available at the link: http://crd.yerphi.am/CORSIKA Simulations 220 221 222 223 **Author contribution** 224 AC and MZ designed the simulation experiments with the CORSIKA code, and LH 225 performed the simulations. AC prepared the manuscript with contributions from all co-226 authors 227 Acknowledgment 228 229 The authors acknowledge the support of the Science Committee of the Republic of 230 Armenia (Research Project No. 21AG-1C012) 231 232 233 References 234 235 236 Alexeenko V.V, Khaerdin.ov N.S, Lidvansky A.S, et al. (2002). Transient variations of 237 secondary cosmic rays due to atmospheric AEF and evidence for pre-lightning particle 238 acceleration. Phys Lett A 301:299-306. 239 240 Ambrozová I., Kákona M., Dvorák R., et al. (2023) Latitudinal effect on the position of Regener-Pfotzer maximum investigated by balloon flight HEMERA 2019 in Sweden and 241 242 balloon flights FIK in Czechia, Radiation Protection Dosimetry 199(15-16), 2041. 243 doi.org/10.1093/rpd/ncac299





- 245 Babich, L. P., Donskoy, E. N., Kutsyk, I. M., & Kudryavtsev, A. Y. (2001). Comparison
- of relativistic runaway electron avalanche rates obtained from Monte Carlo simulations
- and kinetic equation solution. IEEE Transactions on Plasma Science, 29(3), 430-438.

- S. Buitink, H. Falcke, et al. Monte Carlo simulations of air showers in atmospheric AEFs,
- 250 Astropart. Phys. 33 (2010) 1.

251

- 252 Chilingarian A., Mailyan B., and Vanyan L., Recovering the energy spectra of electrons
- and gamma rays coming from the thunderclouds, Atmos. Res. 114–115, 1 (2012).

254

- 255 Chilingarian A., Hovsepyan G., Karapetyan T., et al. (2022), Development of the
- relativistic runaway avalanches in the lower atmosphere above mountain altitudes, EPL,
- 257 139, 50001, https://doi.org/10.1209/0295-5075/ac8763

258

- 259 Chilingarian A., Karapetyan T. Aslanyan D., Sargsyan., B. (2024), Extreme thunderstorm
- ground enhancements registered on Aragats in 2023", Mendeley Data, V1.
- 261 DOI:10.17632/8gtdbch59z. DOI: 10.17632/8gtdbch59z.6

262

- Dwyer J.R. (2003) A fundamental limit on AEFs in air, Geophys. Res. Lett. 30, 2055.
- 264 doi.org/10.1029/2003GL017781

265

- 266 Dwyer G.R., Rassoul H.K. (2024) High energetic radiation from thunderstorms and
- 267 lightning, in Lightning Electromagnetics, IET series Volume 1, 365.

268

- 269 Gurevich, G., Milikh, R., Roussel-Dupre (1992) Runaway electron mechanism of air
- 270 breakdown and preconditioning during a thunderstorm, Physics Letters A 165 (5), 463.

271

- Heck D., Knapp J., Capdevielle J. N., Schatz G., and Thouw T., Report No. FZKA 6019,
- 273 1998, Forschungszentrum, Karlsruhe, https://www.ikp.kit.edu/corsika/70.php.
- 274 Marshall, T. C., M. P. McCarthy, and W. D. Rust (1995), AEF magnitudes and lightning
- initiation in thunderstorms, J. Geophys. Res., 100, 7097.
- 276 Sato, T. Analytical model for estimating the zenith angle dependence of terrestrial cosmic
- 277 ray fluxes. *PLoS ONE* 2016, *11*, e0160390.
- 278 M. Stolzenburg, T. C. Marshall, W. D. Rust, E. Bruning, D. R. MacGorman, and T.
- 279 Hamlin (2007), AEF values observed near lightning flash initiations, Geophys. Res. Lett.,
- 280 34, L04804.

https://doi.org/10.5194/egusphere-2025-4153 Preprint. Discussion started: 5 October 2025 © Author(s) 2025. CC BY 4.0 License.





Symbalisty, E. M. D., R. A. Roussel-Dupré, and V. A. Yukhimuk (1998), Finite volume
 solution of the relativistic Boltzmann equation for electron avalanche studies, IEEE
 Trans. Plasma Sci., 26, 1575–1582.